

# Polyolefin-Based Nanocomposite: The Effects of Processing Aids

K. S. Santos,<sup>1</sup> C. Dal Castel,<sup>1</sup> S. A. Liberman,<sup>2</sup> M. A. S. Oviedo,<sup>2</sup> R. S. Mauler<sup>1</sup>

<sup>1</sup>Instituto de Química, Universidade Federal do Rio Grande do Sul, Av Bento Gonçalves 9500, Porto Alegre-RS 91501-970, Brazil

<sup>2</sup>Braskem S/A, III Pólo Petroquímico, Via Oeste Lote 5, Passo Raso Triunfo, Brazil

Received 29 December 2009; accepted 15 May 2010

DOI 10.1002/app.32828

Published online 19 August 2010 in Wiley Online Library (wileyonlinelibrary.com).

**ABSTRACT:** PP/organoclay nanocomposites were prepared using different processing aids (EMCA and PPG) and their effects on the thermal and mechanical properties were evaluated by WAXD, TEM, SEM, DSC, and mechanical tests. This study helps to clarify the effects of processing aids on the organoclay surface and on the intercalation and exfoliation processes. Nanocomposites with elongated intercalated and partially exfoliated structures were obtained, mainly when C-15A was used. The results for the mechanical properties showed that the processing aids increased the impact strength significantly (up to three times that of neat PP) but reduced the flexural modulus of PP nanocomposites. PPG, which is polar promoted wetting MMT surface, thus increasing its interlayer distance, mainly for PP/C-20A nanocomposites. However, it reduced the interfacial adhesion between the clay and the matrix. Nanocomposites impact strength was

improved, especially when the C-15A organoclay was used, while were achieved better results with the C-20A organoclay when EMCA was used. The larger the amount of processing aid added, the higher the impact strength, but the lower the flexural modulus of the nanocomposites. PPG caused debonding of the clay particles and increased the number of microvoids, generating more mechanisms to aid in the energy dissipation of the systems. EMCA promoted debonding of clay particles with the formation of fibrils, indicating stronger interactions between the clay and matrix. A slight nucleation effect for PP crystallization was observed, mainly when EMCA was used. © 2010 Wiley Periodicals, Inc. *J Appl Polym Sci* 119: 1567–1575, 2011

**Key words:** PP nanocomposites; montmorillonite; thermal properties; morphology

## INTRODUCTION

Polypropylene (PP) is the most widely used thermoplastic due its low cost and attractive properties, such as rigidity, light weight thermal, and chemical stability, but it is relatively brittle at room temperature and exhibits poor resistance to crack-propagation.<sup>1–5</sup>

Compounding with organoclays is a simple, effective, and economical method to improve the mechanical and thermal properties of PP. Many previous studies on organoclay-reinforced polymeric materials have clearly revealed marked improvements in flexural modulus and impact strength, even at low filler loadings of 1–5 wt %, compared to neat PP, independent of the preparation methods.<sup>6–12</sup> The high aspect ratio of the clay layers and the huge interfacial contact area between clay and matrix make this possible.

The complete exfoliation of clay into individual layers optimizes the number of available reinforcing

elements, which increases the matrix rigidity while often decreasing its fracture toughness. It is thought that the size range of clay platelets is too small to provide toughening via mechanisms like multiple crazing, shear yielding, microvoids, and debonding of clay particles. However, an intercalated structure provides better toughening efficiency than a well-exfoliated morphology. On the other hand, large aggregates of clay may serve as stress concentrators that lead to premature brittle failure.<sup>12–22</sup>

To reach a simultaneous improvement in the modulus and impact strength it is necessary to look for alternatives, such as the addition of an elastomeric phase, a compatibilizing agent or blending epoxy resin with polymer/clay nanocomposites.<sup>12</sup> However, it is expensive to obtain such materials. Among these methods, the addition of an elastomeric phase to PP/clay nanocomposites has been the most common method to enhance toughness, but at the expense of stiffness.<sup>12,23–28</sup> A new method that increases the stiffness and the toughness simultaneously is the use of a small amount of a processing aid during the PP/clay nanocomposite synthesis. This type of additive, when incorporated into the PP/clay nanocomposites system, promotes a variation of the interfacial adhesion between the clay and

Correspondence to: R. S. Mauler (raquel.mauler@ufrgs.br).

PP matrix.<sup>29,30</sup> Depending on the chemical nature of the processing aid and the intensity of the clay/PP interface modification, this additive could facilitate clay sheet dispersion in the matrix, decreasing the number of agglomerated structures and the overall properties of the nanocomposites.

The objective of this article is to evaluate the effects of two processing aids, EMCA (apolar character) and PPG (polar character), as well as the effects of the variation of the added amount on the morphology and, consequently, the thermal and mechanical properties of PP/organoclay nanocomposites.

## EXPERIMENTAL

### Materials

Polypropylene homopolymer with a melt flow index (MFI (230°C/2.16 kg)) of 3.5 g/10 min was supplied by Braskem S.A. The antioxidant Irganox® B215 from Ciba was added to the PP. The solvent methyl-ethylketone (MEK) with a density of 0.95 g/cm<sup>3</sup> and a boiling point of 72.11°C from Nuclear; poly(propylene glycol) – PPG, with  $M_n=1000$  g/mol, a viscosity of 190 cP and a density of 1.005 g/cm<sup>3</sup> from Aldrich or EMCA® plus 350 mix; and a paraffin and naphthalene oil, with a viscosity of 129–160cP and a density of 0.8560–0.8780g/cm<sup>3</sup> from Ipiranga S.A were used to prepare a stable suspension with the organophilic montmorillonites: Cloisite® 15A (CEC: 125 meq/100 g) and 20A (CEC: 98 meq/100 g) from Southern Clay Products. The chemical structures of the processing aids (EMCA and PPG) are shown in Figure 1.

### Melt processing

PP nanocomposites were obtained using a twin screw corotating extruder (Haake H-25, model Rheomex PTW 16/25, L/D = 25) operating at 80 rpm. A stable suspension of MMT (5 wt % C-20A or C-15A) and PPG (0, 1, 3 and 10 wt%) or EMCA (1 wt %) in MEK (300 mL) was added into the second feed point, and the residual solvent was removed in the degassing zone as described elsewhere.<sup>31</sup> A temperature range between 170 and 190°C was chosen for the preparation and processing of the nanocomposites to minimize the possible degradation of the organic modifier and the matrix. The nanocomposites were injection-molded as ASTM D-638 Type 1 samples in a Battenfeld Plus 350/075 injection-molding machine. The temperature of the cylinders was kept between 220 and 230°C, and the mold was maintained at 60°C. Films with a thickness of 47 mm were obtained by compression 190°C, and the temperature was maintained for 2 min to obtain a complete melting of the pellets before applying 6 lbs of

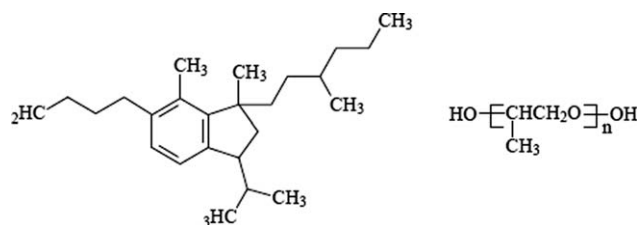


**Figure 1** Chemical structures of the processing aids: (a) EMCA (65% paraffinic carbon, 12% naphthenic carbon and 23% aromatic carbon) and (b) PPG.

pressure for 3 min. The samples were then cooled to room temperature at a cooling rate of  $\sim 20^\circ\text{C}/\text{min}$ . They were used in X-ray and DSC analyses.

### Characterization

WAXD measurements were performed using a Siemens D-500 diffractometer. Film (PP nanocomposites) and powder (organoclays) samples were scanned in the reflection mode using incident  $\text{CuK}_\alpha$  radiation with wavelength of 1.54 Å, at a step width of  $0.05^\circ/\text{min}$  from  $2\theta = 1$  to  $10^\circ$ . The dispersion of the layers in the nanocomposites, and the basal spacing of the clays, was estimated from the (001) diffraction. The morphologies of the specimens were examined by TEM (JEOL JEM-120 Ex II), which was operated at an accelerating voltage of 80 kV. Ultra thin specimens (70 nm) were cut from the middle section of the injection-molded specimens in a direction perpendicular to the flow of the melt during the injection process. Cutting operations were carried out under cryogenic conditions with a Leica Ultracut UCT microtome equipped with a glass or diamond knife at  $-80^\circ\text{C}$ , and the film was placed onto 300 mesh Cu grids. The fracture surface of notched Izod impact specimens (cross section) at room temperature was studied using field emission SEM (JEOL JSM-6060) after coating with platinum to minimize electrostatic charging. The fracture surface morphology of neat PP, PP-clay, and PP-processing aid-clay nanocomposites was observed using an electron accelerating voltage of 10 or 20 kV. Thermal properties were determined using a DSC Thermal Analyst 2100 from TA Instruments. All measurements were carried out under a nitrogen atmosphere. The samples were heated between 50 and  $200^\circ\text{C}$  at a heating and cooling rate of  $10^\circ\text{C}/\text{min}$ . The measurements were made in the second heating and cooling cycles. The degree of crystallinity was determined using  $\Delta H_m^0 = 190$  J/g for PP.<sup>32</sup> The DSC instrument was calibrated with indium before use.

The flexural modulus was measured at room temperature using an Instron 4466 testing machine according to the ASTM D-790 standard at a

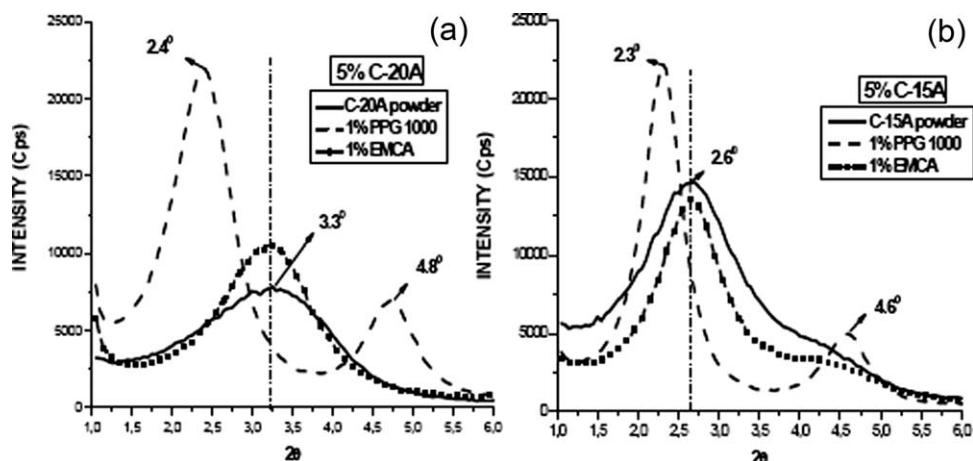


Figure 2 WAXD patterns of the PP/5% organoclays/1% processing aid: (a) C-20A and (b) C-15A.

crosshead speed of 13 mm/min. The notched Izod impact strength was measured using a pendulum-type Ceast 6545 equipment at 23°C with an impact speed of 3.46 m/s according to the ASTM D-256 standard. The reported values were averaged over 10 individual measurements.

## RESULTS AND DISCUSSION

### Clay characterization

The clays were modified with a quaternary ammonium salt with two long alkyl groups with 65% C<sub>18</sub>, 30% C<sub>16</sub>, and 5% C<sub>14</sub>, derived from hydrogenated tallow.<sup>33–35</sup> The difference between the C-20A and C-15A is that the first has 5.6% less organic modifier, and its interlayer distance is 0.7 nm smaller.

The use of PPG displaced the 2θ peak to lower angles (Fig. 2 and Table I), indicating that it penetrated into the silicate sheets due to its more polar character and increased the interlayer distance. It also presented the *d*<sub>002</sub> peak, which was assigned as a second order peak.<sup>29,36–39</sup> The intercalation power of PPG between the MMT layers was 25% larger with the C-20A because its polar surface is less hindered, allowing a stronger interaction with the OH groups present in its structure. In addition, the use of PPG promoted a modification at the PP matrix/MMT interface because it had affinity with the clay surface but not with the PP matrix, decreasing the superficial adhesion between PP and MMT [Fig. 3(a)]. However, the intercalation of the PPG between

the clay sheets reached a maximum of expansion of about 3.7 nm, independent of the clay used. It is believed that the *d*<sub>001</sub> peak disappeared from the X-ray spectrum due to the loss of the structural arrangement of the clay sheets by intercalation with PPG molecules.<sup>36</sup> This effect is not observed with EMCA because it has more affinity with the PP matrix rather than with MMT due to its nonpolar character [Fig. 3(b)].

### Morphology of the PP/organoclay nanocomposites

The nanocomposite morphology is affected by several factors, such as preparation methods, processing conditions, shear stress, matrix molecular weight, structure of the organic modifier, and the compatibilizers used.<sup>6,40–42</sup> Thus, the use of MEK and a processing aid modifies the morphology and consequently the final properties of the PP nanocomposites.

#### PP/C-20A nanocomposites

PP/C-20A nanocomposite morphology with or without MEK exhibited typical aggregates of MMT platelets but few separated clay sheets. The use of solvent should increase the spacing (swelling) between clay layers because of its electric dipolar momentum, which could promote the separation of platelets, but this did not occur, as can be seen in Figure 4.

Elongated structures were formed when PPG was used. It is thought that this processing aid might penetrate into the silicate sheets due to its higher

TABLE I  
Interlayer Distances of the PP/5% Organoclays/1% Processing Aid Nanocomposites

Samples	2θ	<i>d</i> <sub>001</sub> (nm)	Samples	2θ	<i>d</i> <sub>001</sub> (nm)
C-20A	3.3	2.7	C-15A	2.6	3.4
5% C-20A + 1% PPG1000	2.4	3.7	5% C-15A + 1% PPG1000	2.3	3.8
5% C-20A + 1% EMCA	3.3	2.7	5% C-15A + 1% EMCA	2.6	3.4

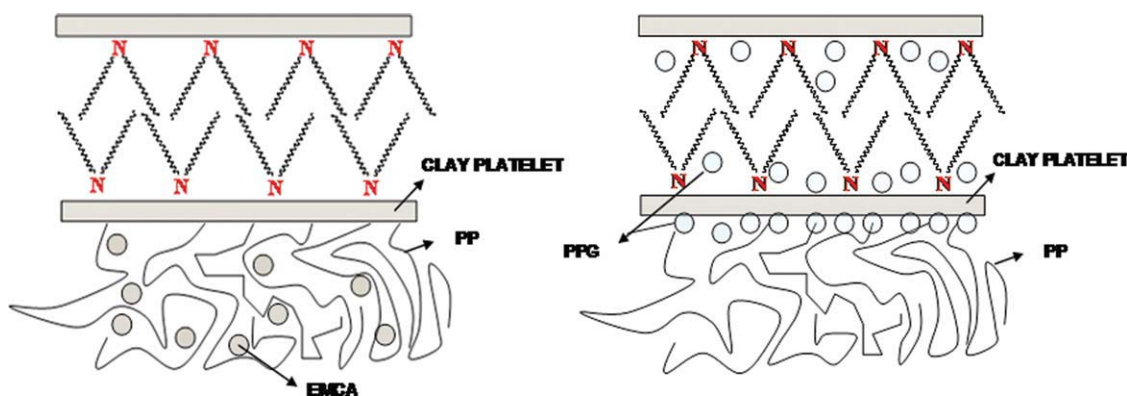


**Figure 3** Sketch of the interactions between PP/organoclay and a processing aid: (a) with EMCA and (b) with PPG. [Color figure can be viewed in the online issue, which is available at [wileyonlinelibrary.com](http://wileyonlinelibrary.com).]

polar character and lower molecular weight, promoting the sliding of the silicate sheets over each other and facilitate the separation of platelets thus decreasing tactoid thickness.<sup>43</sup> In addition, the combination of the diffusion of the polymer chains within the clay galleries and the shear on the platelet surface should promote exfoliation and as such, an increase in the number of individual clay sheets.<sup>29</sup> However, the use of EMCA did not promote the formation of elongated structures. Figure 5 shows the importance of the polarity of the processing aid on the morphology of PP nanocomposites; the polar one improved the MMT dispersion into the PP matrix, while the one did not due to its poor interaction with MMT.

The use of a larger amount of PPG (3 wt %) reduced the number and size of aggregates of MMT platelets drastically, promoting an increase in the number of elongated intercalated structures with greater separation between platelets. This effect can be verified by comparing Figures 5(a) and 6. The larger the amount of PPG, the higher the degree of “swelling” of the clay.

PP/C-15A nanocomposites

The use of C-15A, which has larger amounts of organic modifier, led to nanocomposites with fewer agglomerated structures. It is believed the reason for this behavior can be associated with the larger platelets separation provided by the larger amount of surfactant in this organoclay. This behavior is independent of the use of EMCA or PPG. However, elongated structures were formed only when PPG was used [Fig. 7(b)]. The structural arrangements were different from those presented for the same system using C-20A (Figs. 5 and 7). The system with C-15A presented a higher aspect ratio, with a higher length and lower tactoid thickness.

#### Relationship between morphology and thermal properties

The crystallization behavior and the crystalline morphology of nanocomposites are strongly affected by the presence of the layered silicates and their

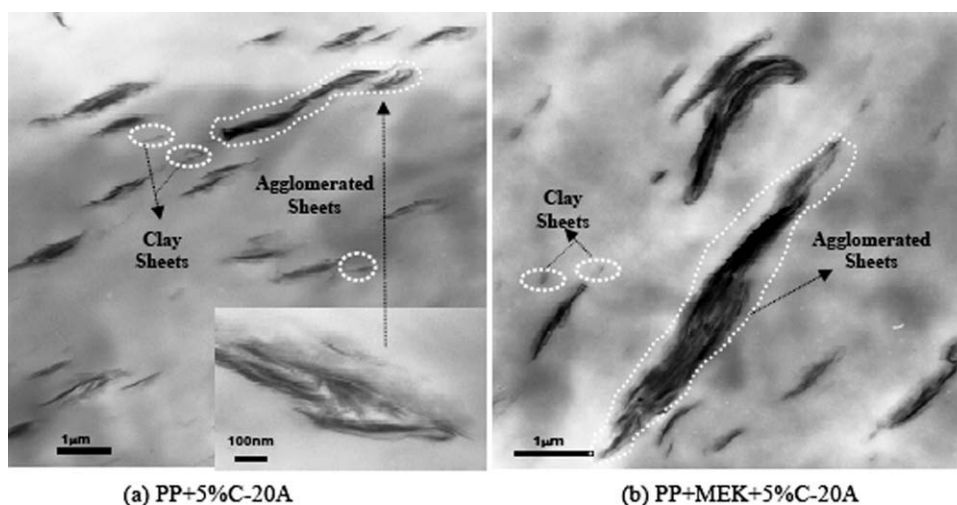


**Figure 4** TEM images of PP/5%C-20A nanocomposites: (a) without MEK and (b) with MEK.

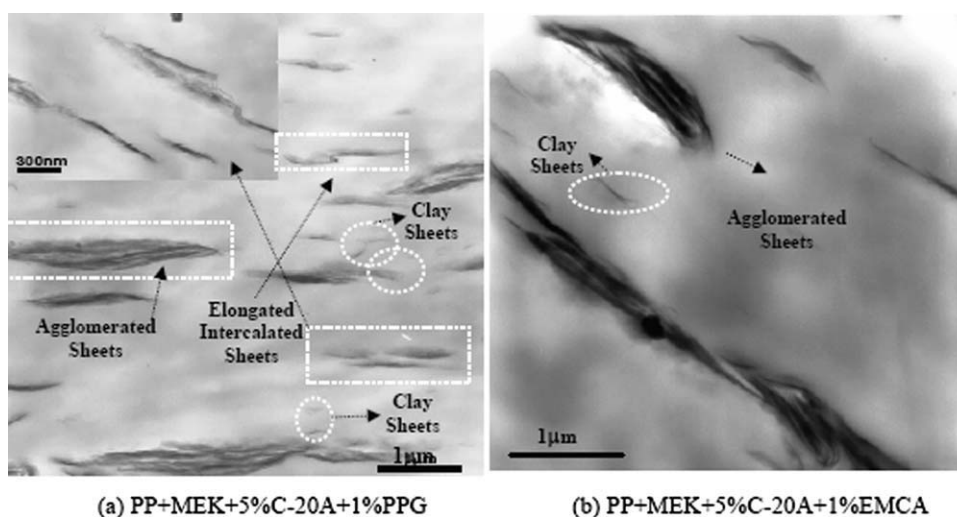


Figure 5 TEM images of PP/5%C-20A nanocomposites: (a) 1% PPG and (b) 1% EMCA.

morphology. The better the clay dispersion into the matrix, the larger the number of nuclei formed and, consequently, the higher the crystallization temperature. Heterogeneous nucleation has been observed in polymeric nanocomposites by several researchers.<sup>2,14</sup> The organoclay increases the nanocomposite crystallization temperature ( $T_c$ ) because it acts as a nucleation agent, promoting matrix crystallization. This behavior promotes changes in crystal structure that may influence the reinforcement ability of the silicates in nanocomposites. The presence of clay or the addition of EMCA or PPG as a processing aid did not influence either  $T_m$  or  $X_c$ , despite the fact that the  $T_c$  was shifted to higher temperatures with clay content (Table II). The crystallization temperature of neat PP is about 113°C, while the crystallization temperature with 5 wt % clay is about 118°C. The use of PPG and EMCA as a processing aid affects the nucleation behavior of the clay differently. In the case of EMCA oil, which is less polar and has poor interaction with the clay, some nucleation was observed. However, the use of PPG did not induce the nucleation, probably because it wet the clay and prevented the MMT/PP interaction.

#### Relationship among fractography, morphology, and mechanical properties

As shown in Table II, the presence of MEK in the process caused a slight increase in the impact strength of PP (from 34 to 51 J/m) because it increased the free volume of the polymer chains, thus reducing the flexural modulus of the matrix. The addition of EMCA did not change this behavior. On the other hand, the addition of PPG + MEK did not influence the flexural modulus of PP, but it increased the impact strength of matrix, indicating a lower plasticizer effect. The addition of 5% C-20A,

without the use of a processing aid or MEK, caused a remarkable increase in the flexural modulus but with a lower increase in the impact strength. The use of MEK with the clay maintained the impact strength and reduced the flexural modulus, but it remained superior to that of neat PP. The use of a processing aid in the PP/clay/MEK systems promoted significant improvements in the impact strengths (up to three times more than that of neat PP). However, the flexural modulus was only slightly higher than that of neat PP. Impact strength increased and flexural modulus decreased with increasing amount of processing aid. C-20A systems displayed better properties when EMCA was used while for C-15A systems, the processing aid which

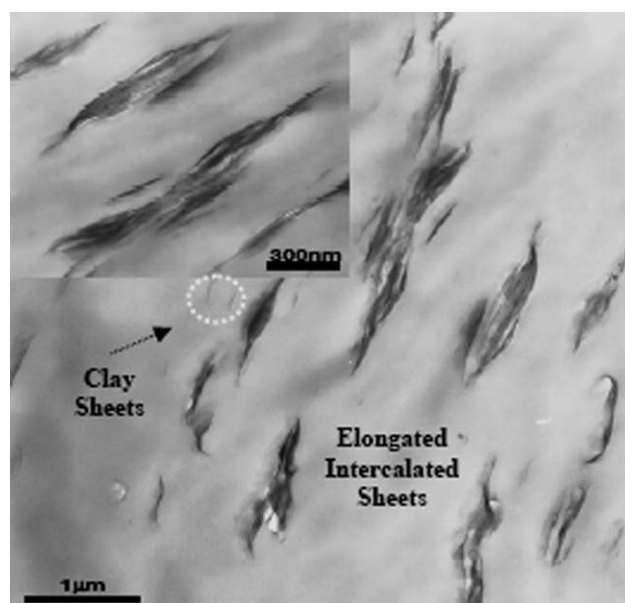


Figure 6 TEM images of PP/5%C-20A/3% PPG nanocomposites.

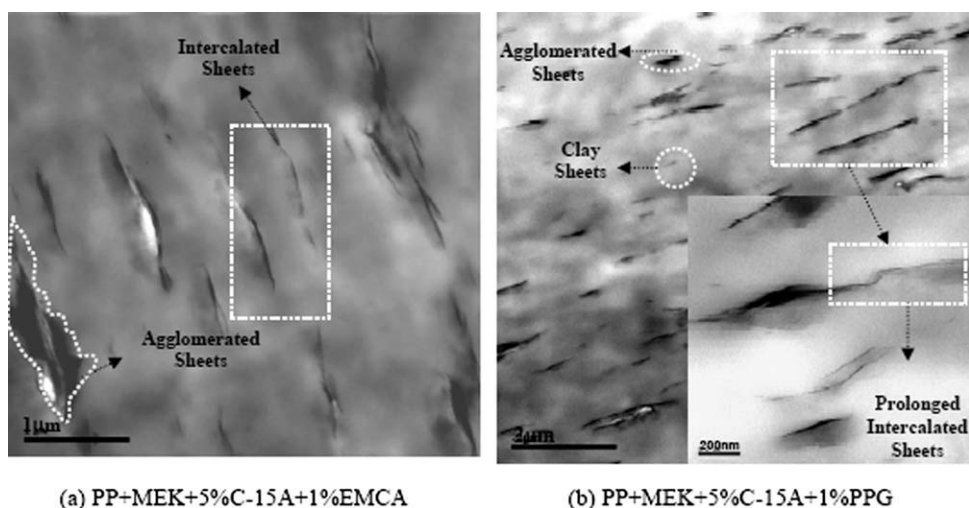


Figure 7 TEM images of PP/5%C-15A nanocomposites: (a) 1% EMCA and (b) 1% PPG.

helped to enhance performance was PPG. It is believed the reason for this behavior is that the energy barrier to reduce the sheet-sheet interaction of C-20A is larger than that of C-15A, C-20A has a smaller amount of organic modifier between its layers, and this means that it is surface free to interact with PPG, which eventually covers the clay surface, reducing the surface-clay/matrix interaction.<sup>29</sup> Thus, the interfacial adhesion between C-20A/PP is reduced, decreasing the PP nanocomposite mechanical properties.<sup>14</sup> When EMCA was used this effect was minimized because this processing aid penetrates into the empty spaces of the polymer chains and decreases the intermolecular force, favoring the interaction of the polymer chain with the organoclay. PPG has a weak interaction with the C-15A surface because the surface of this clay is more hindered by the larger amount of surfactant. As a result

this processing aid acts as a filler into the layers, facilitating the sliding of the sheets over one another and allowing a larger interaction of clay/PP, which leads to more effective elongated structures. The fractography of the impact fracture surfaces of pristine PP, PP+MEK, and PP nanocomposites using PPG or EMCA helps to better understand the effects of these processing aids on the impact strength of these materials. This property is influenced by the type of particles, the morphology, and the variation in the interfacial adhesion between the clay and matrix. Thus, the larger the impact strength, the larger the plastic deformation of the matrix. However, to have a larger plastic deformation, a weak interaction between the clay platelets and a stronger interaction between the clay and the matrix is necessary, in addition to a good dispersion and orientation of the clay sheets in the matrix.<sup>20,44,45</sup> In clay-

TABLE II  
Mechanical and Thermal Properties of the PP Nanocomposites

Samples	Flexural modulus (MPa)	Impact izod 23°C (J/m)	$T_m^a$ (°C)	$T_c^a$ (°C)	$X_c$ (%)
BLANKS					
Neat PP	1416 ± 17	34 ± 2	164	113	53
Neat PP + MEK	1251 ± 28	51 ± 6	163	113	57
Neat PP + MEK + 1%PPG	1459 ± 5	49 ± 7	–	–	–
Neat PP + MEK + 1%EMCA	1258 ± 8	56 ± 5	–	–	–
Without processing aid					
PP + 5%C-20A	1907 ± 14	48 ± 5	163	116	54
PP + MEK + 5%C-20A	1689 ± 33	46 ± 1	164	116	51
PPG					
PP + MEK + 5%C-20A + 1%PPG	1556 ± 13	58 ± 4	162	114	45
PP + MEK + 5%C-20A + 3%PPG	1518 ± 22	72 ± 8	164	114	51
PP + MEK + 5%C-20A + 10%PPG	1440 ± 34	106 ± 6	163	113	50
PP + MEK + 5%C-15A + 1%PPG	1563 ± 17	82 ± 4	164	115	49
EMCA					
PP + MEK + 5%C-20A + 1%EMCA	1650 ± 21	72 ± 10	164	118	50
PP + MEK + 5%C-15A + 1%EMCA	1401 ± 21	62 ± 3	163	116	55

<sup>a</sup> standard deviation ± 1°C.

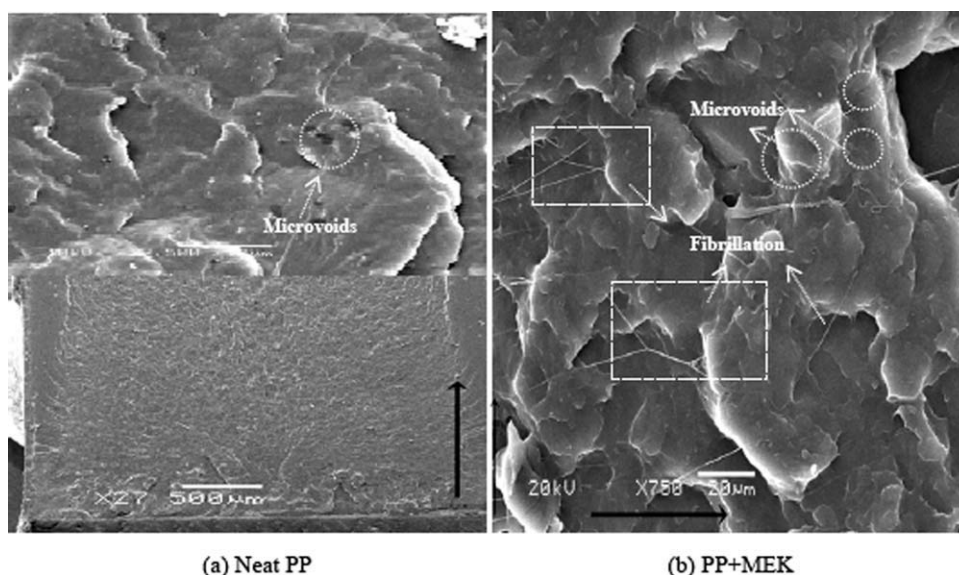


**Figure 8** SEM micrograph of the impact fracture surface: (a) neat PP and (b) PP+MEK.

reinforced semicrystalline thermoplastic nanocomposites, microdeformation processes, identified as energy dissipating mechanisms, include crazing, cavitation and the debonding of clay particles with consequent microvoid formation with or without fibrillation, which cause the posterior shear yielding of the matrix.<sup>20,44,46,47</sup> The great flexibility of the clay platelets allows for curvature and facilitates plastic deformation through microvoid formation in the layers.<sup>30</sup> The microvoid formation occurs by cavitation or debonding of clay particles and by the breaking, opening, or sliding of the platelets. Thus, the increase in the number of microvoids with elongated structure will increase the energy absorption by the

shear yielding process.<sup>14,44</sup> SEM micrographs of pristine PP, PP+MEK, and PP nanocomposites using PPG or EMCA visibly support this argument. The crack-propagation direction is indicated with a black arrow in the micrographs. The crack-propagation profiles of the materials are omitted because the energy dissipation mechanisms are observed at larger SEM image magnification, and only close-up views of these profiles are shown in Figures 8–13.

The fractured surface of the pristine PP presented predominantly craze-like features with a small number of microvoids, while the use of MEK increased the number of microvoids with a fibrillation net, producing a positive effect on the energy dissipation

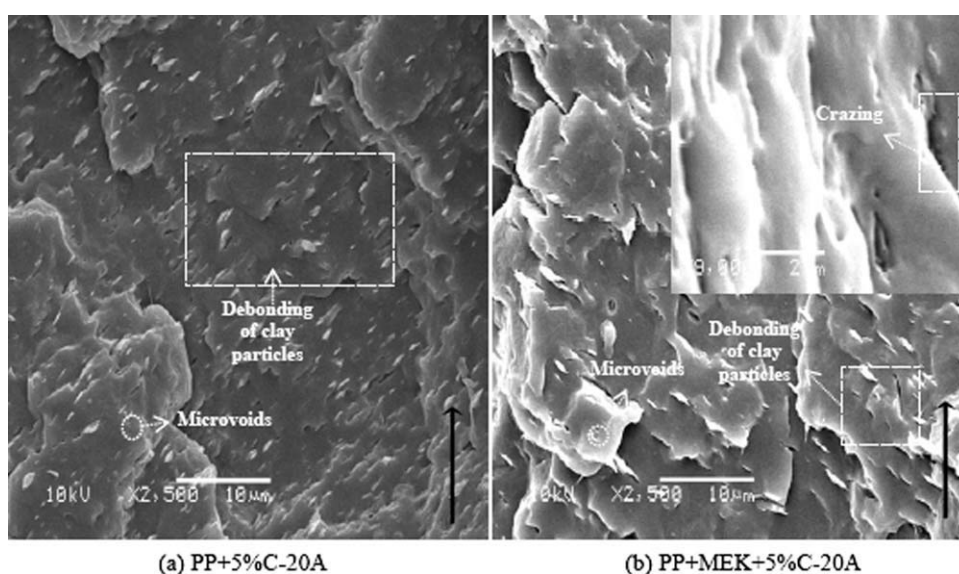


**Figure 9** SEM micrograph of the impact fracture surface of PP/5%C-20A nanocomposites: (a) without MEK and (b) with MEK.

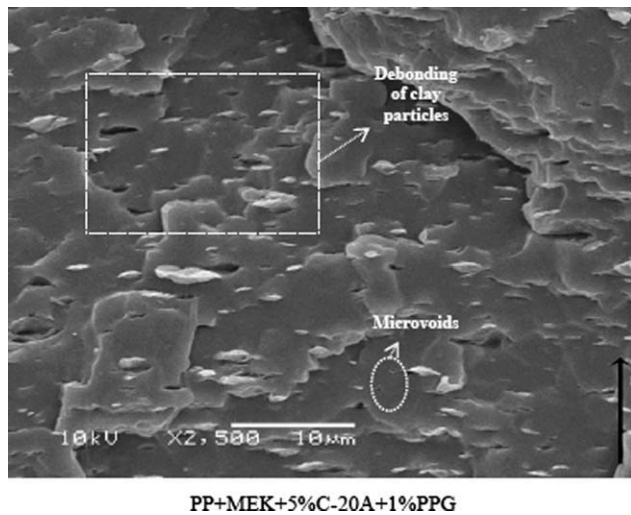


**Figure 10** SEM micrograph of the impact fracture surface of PP/C-20A nanocomposites: 1% PPG.

mechanisms [Fig. 8(a,b)]. The systems with 5% C-20A with or without MEK presented microvoids with reduced size and number of microfibrils and debonded clay particles  $\sim 1 \mu\text{m}$  in size [(Fig. 9(a,b))].

When 1 wt % PPG was used the size of the debonded clay particles was increased to 2–3  $\mu\text{m}$ , showing an elongated structure (Fig. 10). The increase in PPG (3 wt %) increased the number of microvoids and elongated structures, resulting in an increase of the impact strength (Fig. 11).<sup>45</sup> The use of EMCA promoted a similar behavior with 5% C-20A with or without MEK; however, the debonding of clay particles presented fibrils, indicating stronger interactions between the clay and the matrix. With PPG, this behavior was not observed. Furthermore, this system presented another energy dissipation mechanism responsible for microvoid formation: the

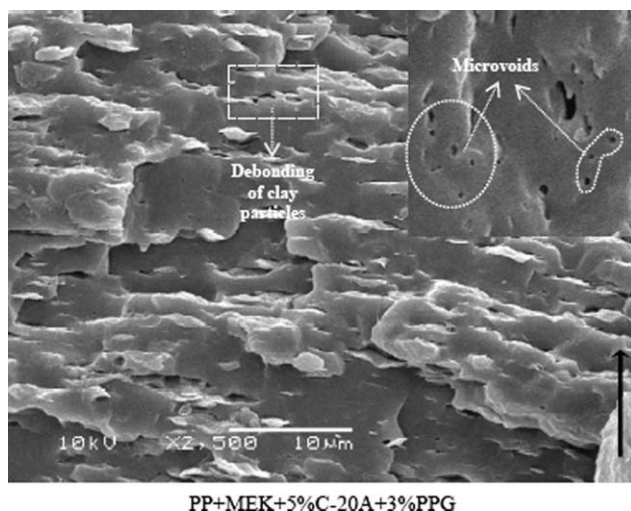


**Figure 11** SEM micrograph of the impact fracture surface of PP/C-20A nanocomposites: 3% PPG.

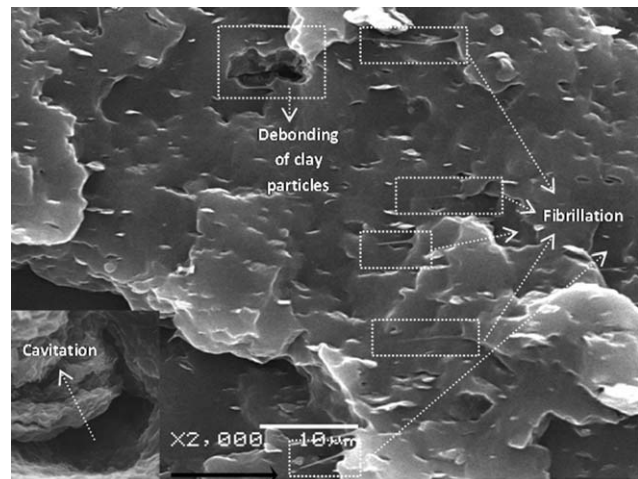


**Figure 12** SEM micrograph of the impact fracture surface of PP/C-20A nanocomposites: 1% EMCA.

cavitation mechanism (Fig. 12). Cavitation in the amorphous region releases plastic constraints and allows the plastic deformation of the matrix.<sup>1,14,48</sup> This behavior proves that EMCA interacts only with the PP matrix, increasing its amorphous regions. When C-15A was used with PPG in the same conditions as the C-20A the behavior was similar but with a higher number of microvoids. Besides, it was possible to observe the coalescence of the microvoids, generating larger energy dissipation in the system (Fig. 13).

## CONCLUSION

PP nanocomposites were prepared using different processing aids.  $T_m$  and  $X_c$  were not almost affected by the presence of clay, MEK solvent, or processing aids. A slight nucleation of PP crystallization was

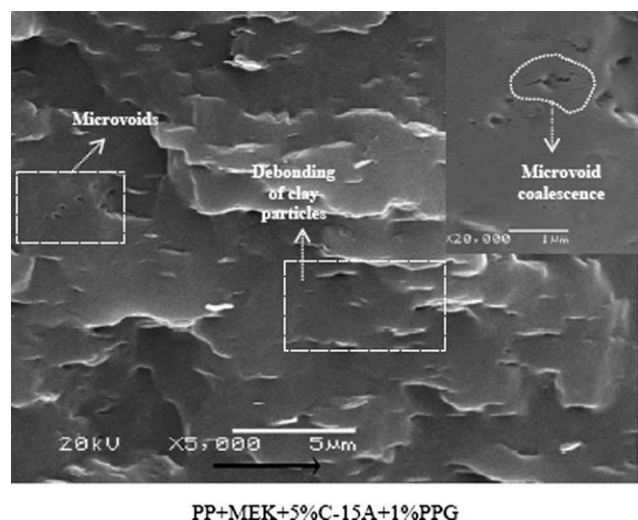


**Figure 13** SEM micrograph of the impact fracture surface of PP/C-15A nanocomposites: 1% PPG.



observed, mainly when EMCA was used. The use of a processing aid modifies the interface between the clay and matrix and consequently the final properties, increasing the impact strength significantly (up to three times more than that of neat PP), but it has a minimal effect on the flexural modulus of the PP nanocomposites. The polarity of the processing aid is directly related to the intensity of the interfacial adhesion between the clay surface and the PP matrix. PPG, which is polar, promoted the wetting of the MMT surface, increasing its interlayer distance. In addition, it induced the formation of elongated intercalated structures but reduced the interfacial adhesion between the clay and matrix, mainly with C-20A nanocomposites. EMCA, which is nonpolar, reduced the interaction between the PP chains, facilitating the interaction between PP and clay. PPG produced more improvement in the impact strength when C-15A was used, while EMCA presented better results with C-20A. The larger the amount of processing aid, the higher the impact strength, but the flexural modulus was only slightly affected. When PPG was used, debonding of clay particles and the number of microvoids increased, generating more mechanisms that aid in the energy dissipation of the system, while EMCA promoted the debonding of clay particles with fibril formation, indicating stronger interactions between the clay and matrix.

The authors are grateful to CAPES, CNPq, Finep, and FAPERGS/PRONEX for their financial support.

## References

- Lin, Y.; Chen, H.; Chan, C.-M.; Wu, J. *Macromolecules* 2008, 41, 9204.
- Yuan, Q.; Misra, R. D. K. *Polymer* 2006, 47, 4421.
- Elmajdoubi, M.; Vu-Khanh, T. *J Theor Appl Fract Mech* 2003, 39, 117.
- Thio, Y. S.; Argon, A. S.; Coehn, R. E.; Weinberg, M. *Polymer* 2002, 43, 3661.
- Van Der Wal, A.; Mulder, J. J.; Thijs, H. A.; Gaymans, R. J. *Polymer* 1998, 39, 5467.
- Rohlmann, C. O.; Horst, M. F.; Quinzani, L. M.; Failla, M. D. *Eur Polym J* 2008, 44, 2749.
- Kornmann, X.; Lindberg, H.; Berglund, L. A. *Polymer* 2001, 42, 1303.
- Agag, T.; Koga, T.; Takeichi, T. *Polymer* 2001, 42, 3399.
- Nam, P. H.; Maiti, P.; Okamoto, M.; Kotaka, T.; Hasegawa, N.; Usuki, A. *Polymer* 2001, 42, 9633.
- Rhoney, I.; Brown, S.; Hudson, N. E.; Pethrick, R. A. *J Appl Polym Sci* 2004, 9, 1335.
- Alexandre, M.; Dubois, P. *Mater Sci Eng R* 2000, 28, 1.
- Yu, Z.-Z.; Dasari, A.; Mai, Y.-W. In *Processing and Properties of Nanocomposites*; Advani, S. G., Ed. World Scientific Publishing: Singapore, 2007; p 310.
- Zuiderduin, W. C. J.; Westzaan, C.; Huétink, J.; Gaymans, R. J. *Polymer* 2003, 44, 261.
- Tanniru, M.; Yuan, Q.; Misra, R. D. K. *Polymer* 2006, 47, 2133.
- Haworth, B.; Raymond, C. L.; Sutherland, I. *Polym Eng Sci* 2001, 41, 1345.
- Hadal, R. S.; Misra, R. D. K. *Mater Sci Eng A* 2004, 374, 374.
- Yuan, Q.; Jiang, W.; Zhang, H. Z.; Yin, J. H.; An, L. J.; Li, R. K. Y. *J Polym Sci Part B: Polym Phys* 2001, 39, 1855.
- Dasari, A.; Misra, R. D. K. *Acta Mater* 2004, 52, 1683.
- Tanniru, M.; Misra, R. D. K.; Bertrand, K.; Murphy, D. *Mater Sci Eng A* 2005, 404, 208.
- Kim, G. M.; Michler, G. H. *Polymer* 1998, 39, 5699.
- Wu, J. S.; Yu, D. M.; Mai, Y. W.; Yee, A. F. *J Mater Sci* 2000, 35, 307.
- Kim, G. M.; Lee, D. H.; Hoffmann, B.; Kressler, J.; Stoppelmann, G. *Polymer* 2001, 42, 1095.
- Dasari, A.; Yu, Z. Z.; Yang, M.; Zhang, Q. X.; Xie, X. L.; Mai, Y.-W. *Comp Sci Technol* 2006, 66, 3097.
- Khatua, B. B.; Lee, D. J.; Kim, H. Y.; Kim, J. K. *Macromolecules* 2004, 37, 2454.
- Liu, X. H.; Wu, Q. J.; Berglund, L. A.; Fan, J. Q.; Qi, Z. N. *Polymer* 2001, 42, 8235.
- Chow, W. S.; Baker, A. B.; Ishak, Z. A. M.; Karger-Kocsis, J. *Eur Polym J* 2005, 41, 687.
- Liu, X. H.; Wu, Q. J. *Macromol Mater Eng* 2002, 287, 180.
- Wang, Y.; Zhang, Q.; Fu, Q. *Macromol Rapid Commun* 2003, 24, 231.
- Carretero-González, J.; Valentín, J. L.; Arroyo, M.; Saalwächter, K.; Lopez-Manchado, M. A. *Eur Polym J* 2008, 44, 3493.
- Wang, K.; Liang, S.; Deng, J.; Yang, H.; Zhang, Q.; Dong, X.; Wang, D.; Han, C. C. *Polymer* 2006, 47, 7131.
- Lieberman, S.; Da Silva, L.; Pelegrine, T.; Barbosa, R.; Mauler, R. Pat. No. W02007009200-A2; BR200503777-A, 2007.
- Amash, A.; Zugenmaier, P. *J Appl Polym Sci* 1997, 63, 1143.
- Útracki, L. A. *Clay-Containing Polymeric Nanocomposites*; Rapra Technology: Shawbury, 2004.
- Leszczynska, A.; Njuguna, J.; Pielichowski, K.; Banerjee, J. R. *Thermochim Acta* 2007, 453, 75.
- Leszczynska, A.; Njuguna, J.; Pielichowski, K.; Banerjee, J. R. *Thermochim Acta* 2007, 454, 1.
- Santos, K. S.; Liberman, A. S.; Oviedo, M. A. S.; Mauler, R. S. *J Polym Sci Part B: Polym Phys* 2008, 46, 2519.
- Harris, J.; Bonagamba, T. J.; Schmidt-Rohr, K. *Macromolecules* 1999, 32, 6718.
- Paul, D. R.; Robeson, L. M. *Polymer* 2008, 49, 3187.
- Pozsgay, A.; Fráter, T.; Százdí, L.; Müller, P.; Sajó, L.; Pukanszky, B. *Eur Polym J* 2004, 40, 27.
- Benetti, E. M.; Causin, V.; Marega, C.; Marigo, A.; Ferrara, G.; Ferraro, A.; Consalvi, M.; Fantinel, F. *Polymer* 2005, 46, 8275.
- Perrin-Sarazin, F.; Ton-That, M.; Bureau, M.; Denault, J. *Polymer* 2005, 46, 11624.
- Li, J.; Ton-That, M. T.; Tsai, S. J. *Polym Eng Sci* 2006, 46, 1060.
- Santos, K. S.; Liberman, A. S.; Oviedo, M. A. S.; Mauler, R. S. *Compos A* 2009, 40, 1199.
- Sun, L.; Gibson, R. F.; Gordaninejad, F.; Suhr, J. *Compos Sci Technol* 2009, 69, 2392.
- Miyagawa, H.; Drzal, L. T. *J Adhes Sci Technol* 2004, 18, 1571.
- Ha, S. R.; Rhee, K. Y.; Kim, H. C.; Kim, J. T. *Colloid Surf A: Physicochem Eng Aspects* 2008, 313, 112.
- Wang, K.; Chen, L.; Wu, J. S.; Toh, M. L.; He, C. B.; Yee, A. F. *Macromolecules* 2005, 38, 788.
- Michler, G. H.; Adhikari, R.; Henning, S. *J Mater Sci* 2004, 39, 3281.